New evidence for sedimentary volcanism on Chryse Planitia, Mars

P. Brož, E. Hauber, S. J. Conway, E. Luzzi, A. Mazzini, A. Noblet, J. Jaroš, P. Fawdon, Y. Markonis

New evidence for sedimentary volcanism on Chryse Planitia, Mars

P. Brož[1*], E. Hauber[2], S. J. Conway[3], E. Luzzi[4], A. Mazzini[5], A. Noblet[3], J. Jaroš[6] , P. Fawdon[7], and Y. Markonis[6]

[1] Institute of Geophysics of the Czech Academy of Science, Boční II/1401, 141 31, Prague, Czech Republic.

[2] Institute of Planetary Research, DLR, Rutherfordstr. 2, 12489, Berlin, Germany.

[3] Nantes Université, Université d'Angers, Le Mans Université, CNRS UMR-6112 Laboratoire de Planétologie et Géosciences, France.

[4] Jacobs University Bremen, Campus Ring 1, 28759, Bremen, Germany.

[5] Centre for Earth Evolution and Dynamics (CEED), University of Oslo, Norway.

[6] Faculty of Environmental Sciences, Czech University of Life Sciences Prague, Czech Republic.

[7] School of Physical Sciences, Open University, Milton Keynes, Buckinghamshire, MK7 6AA, United Kingdom

Corresponding author: Petr Brož (petr.broz@ig.cas.cz)

Abstract

Kilometre-sized flows (KSFs) have been observed in many regions on Mars and have been typically interpreted as lava flows. However, sedimentary volcanism has been proposed as an alternative origin for some KSFs. Remarkable examples of such hypothesized sedimentary KSFs are located at the southern margin of Chryse Planitia. There, the flows are associated with conical and dome-shaped edifices, however their formation mechanism remained enigmatic due to the absence of ground truth. Here, we present new morphological results obtained on these KSFs using seven newly available Digital Elevation Models computed from HiRISE stereo pairs. Our investigation confirms that these features are aggradational and formed by the transport of a liquid. This material emerged from identified depressions and the presence of subtle mounds inside them is interpreted to mark the position of feeder vents. We also observe that the margins surrounding the central large channels are not continuous. They are cut by meter-sized troughs linking the central channels to units with distinctive albedo and roughness from their surroundings. These bright units do not have a clear topographical expression, suggesting that the effused material originally flowing away from the central channel was easily removed after its emplacement. Such surface features are unlikely to be related to igneous deposits, since once lava is released from a main channel, it would rapidly solidify due to the heat loss and hence result in topographically distinct features. In contrast, such morphological expressions are more likely related to sedimentary volcanism and the emplacement of low viscosity water-rich mud. Sublimation, evaporation, infiltration or a combination of these processes should lead to water loss without leaving a detectable topographic expression but changing the roughness and hence albedo of the surface. The southern part of Chryse Planitia is a region on Mars where subsurface sediment mobilization operated in the past and hence represents a promising site for future exploration where deeper-sourced sedimentary deposits are exposed at the surface.

1 Introduction

High-resolution images have revealed the presence of kilometre-sized flows (KSFs) on Mars. Most of these features are associated with well-known volcanic centres, such as Tharsis, Elysium or Syrtis Major, and therefore have been interpreted as lava flows (e.g., Hodges & Moore, 1994; Bleacher et al., 2007; Keszthelyi et al., 2008; Hauber et al., 2009). Some KSFs, however, occur in regions where a direct link to magmatic activity is not obvious, and an alternative formation scenario related to sedimentary volcanism has been proposed (Wilson and Mouginis-Mark, 2014; Okubo, 2016; Komatsu et al., 2016; Brož et al., 2019). This mechanism has been challenged because the current martian atmospheric pressure is considered too low to allow water to be stable for prolonged periods of time at the surface. If liquid water were exposed on the martian surface today, it would boil and eventually evaporate into the atmosphere, and therefore mud flows, similar to the terrestrial ones, are not supposed to occur (e.g., Hecht, 2002; Bargery et al., 2010). Therefore, it remains unclear if mud would be able to propagate on Mars` surface via mud flows under the current atmospheric pressure.

Several studies (e.g., Wilson and Mouginis-Mark, 2014; Brož et al., 2020a,b) have recently shown that the instability of water within the mud is a critical factor which could affect the way that mud propagates over the martian surface. These results show that evaporative cooling would cause the mixture to freeze (Bargery et al., 2010). However, this process would occur only at the flow's surface (Brož et al., 2020a). Consequently, the mud flow's interior could remain liquid for prolonged periods of time allowing lateral propagation while "protected" by an icy-muddy crust (Brož et al., 2020a). Therefore, sedimentary volcanism on Mars should exhibit observational evidence that can be identified on the surface, although its precise morphology should differ from mudflows on Earth.

A remarkable example of KSFs accompanied by conical and dome-shaped edifices was reported by Komatsu et al. (2016) from the southern margin of Chryse Planitia on Mars (19.16°N; 322.71°E), at the terminations of the large outflow channels of Simud, Tiu and Ares Valles formed during the Hesperian epoch (Tanaka et al., 2005). Komatsu et al. (2016) proposed that these KSFs were resulted

from subsurface sediment mobilization. This conclusion holds on the observation that the studied edifices have morphological and morphometrical similarities with terrestrial mud flows. However, similar morphologies and morphometries could also develop during the emplacement of low viscosity lava flows. Brož et al. (2019) later identified thirty-five similar KSFs as part of large, >1,300 population of dome-shaped, conical, pie-like and flow-like edifices mapped exclusively on sedimentary plains. The authors argued for a genetic link between these features and the associated sedimentary units. Such distinct coupling favours sedimentary volcanism over igneous volcanism as a potential genetic mechanism, although the latter could not be ruled out.

Komatsu et al. (2016) and Brož et al. (2019) showed that KSFs at the southern margin of Chryse Planitia typically consist of three morphological elements: a) a central depression from which one or more channels originate, b) leveed channels, c) a distal portion of the fading channel(s) where the material is deposited forming terminal lobes. Based on these morphologies, Brož et al. (2019) later proposed that these KSFs resulted from low viscosity mud extrusions that propagate through channels, gradually losing their transport energy. Without data on the composition and internal structure of the KSF, this hypothesis could not be fully substantiated. The initial studies used images from the Context Camera (CTX) (~5-6 m/px, Malin et al., 2007) and High Resolution Imaging Science Experiment (HiRISE) (~30 cm/px; McEwen et al., 2007), and lacked topographic data to support their inferences. Six KSFs are now covered by HiRISE stereo pairs (Fig. 1) enabling us to generate seven Digital Elevation Models (DEMs) with a ground sampling distance of 1-2 m/px. These new data provide additional details about the shapes of KSFs and new information to validate or disprove whether the observed morphologies are consistent with a sedimentary volcanism scenario.

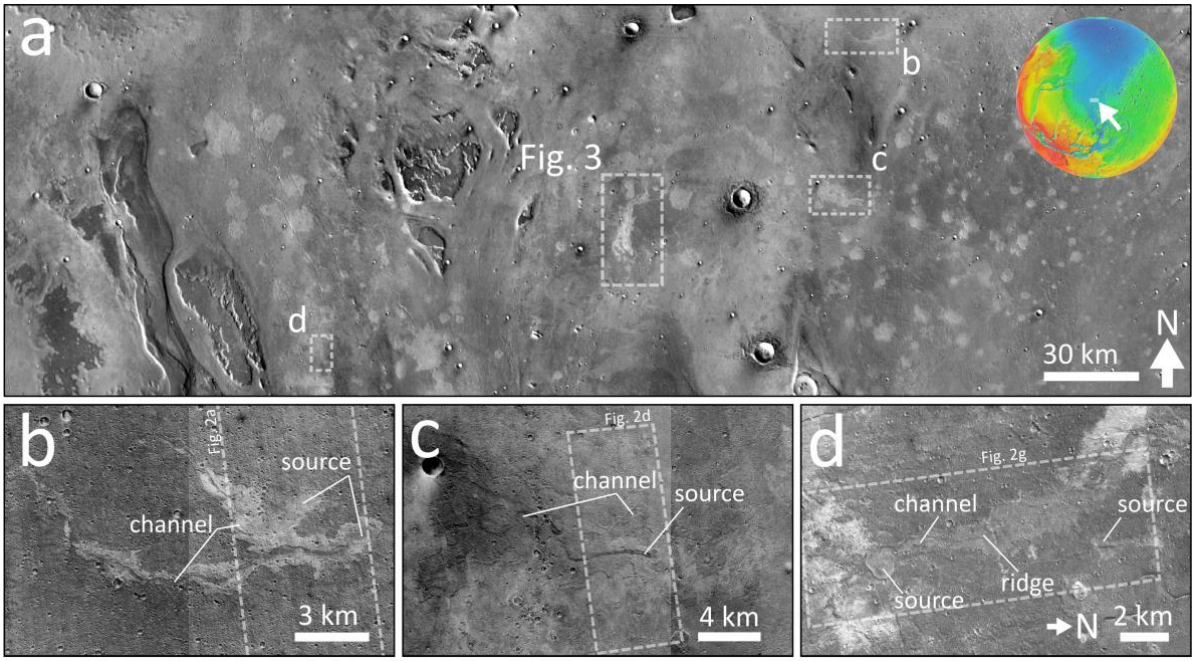

Figure 1: Location of investigated KSFs in Chryse Planitia. (a) THEMIS-IR nighttime image of study area that hosts a large assemblage of surficial features interpreted as sedimentary volcanoes by Komatsu et al. (2016) and Brož et al. (2019), visible as light-toned units on the lowlands. Image centred at 19.25°N and 322.34°E. Inset globe, indicating the location of the study area, is based on colourised MOLA topographic data (blue=low elevation, red=high). The location of the kilometre-sized flows described in this study are marked on panels (b-d) and on Figure 3. The dashed lines in panels (b), (c), and (d) mark the position of HiRISE stereo-pairs that are shown in Figure 2. Panels (b), (c) and (d) are based on the Murray Lab CTX mosaic (Dickson et al., 2018).

2 Data and methods

This study uses data obtained by two cameras; CTX (Malin et al., 2007) and HiRISE (McEwen et al., 2007), both on board NASA's Mars Reconnaissance Orbiter spacecraft. The resolution of the CTX images is around ~6 m/pixel, and for HiRISE images ~30 cm/pixel. While the CTX data were used to provide context and study the wider surroundings of KSFs, the newly available HiRISE stereo-pairs were used to compute the high-resolution DEMs. Seven HiRISE DEMs were produced by using the standard workflow using the software packages ISIS3 and ®BAE Systems SOCET SET. The images of the stereo pairs were first manually co-registered to perform a bundle adjustment, then automatic extraction of the relief was performed using SOCET SET. The DEMs were vertically controlled to Mars Orbiter Laser Altimeter (MOLA) elevation data. The vertical precision of the DTMs is estimated as: maximum resolution/5/tan (convergence angle) (Kirk et al, .2008). CTX and HiRISE images together

with the DEMs were then analysed in the ESRI ArcGIS 10 software including extraction of topographic profiles. Topographic information was obtained by using the 3D Analyst and Spatial Analyst tools within this software. An estimation of general slope of areas where KSFs were identified was made by calculating a slope map. To generate the slope map a plane is fitted to the 3x3 neighbourhood surrounding each pixel in the DEM and its slope calculated (Burrough and McDonell, 1998). Two separate locations within the study area were defined for this slope analysis. The data were projected in an Equirectangular Map projection with the central meridian set at 180°E.

DEM	HiRISE Image 1	Pixel Scale image 1 (m)	HiRISE Image 2	Pixel Scale image 2 (m)	Convergence angle (°)	Ground-sampling dimension (m)	Vertical precision (m)
Chryse (1)	ESP_064644_1990	0.29	ESP_065488_1990	0.28	13.4	1	0.24
Chryse (2)	ESP_065356_1995	0.57	ESP_065422_1995	0.58	17.8	2	0.36
Chryse (3)	ESP_024082_1995	0.57	ESP_023581_1995	0.6	26.2	2	0.23
Chryse (4)	ESP_025071_1995	0.57	ESP_025137_1995	0.62	30.2	2	0.20
Chryse (5)	ESP_067150_2005	0.57	ESP_068034_2005	0.65	38.1	2	0.15
Chryse (6)	ESP_020469_1995	0.29	ESP_037598_1995	0.29	14.5	1	0.22
Chryse (7)	ESP_064156_2005	0.29	ESP_064868_2005	0.29	26.7	1	0.12

Table 1: Details about used HiRISE stereo-pairs, their vertical precision and the software used for their preparation.

3 Observations

The studied KSFs can be clearly distinguished in topographic data. They show a topographically well-defined “source” area with circular, semi-circular or elongated map-view outline (Figs. 1, 2a). Three source areas are situated on relatively flat plains and are surrounded by elevated, several hundred-meter-wide rims (Fig. 2d). The other source areas are superposed on higher elevation and inclined pre-existing surfaces with less laterally extensive rims (Fig. 1). The elevation difference between source

125 area floors and the rims ranges from 10 to 20 m. The elevation of the source area floors is the same as
126 that of the plains beyond the elevated margins on which the KSFs are superposed. The margins of all
127 studied source areas are breached (Figs. 2b, e, h, 3b), presumably enabling the extruded fluid to flow
128 out and propagate resulting in the formation of the observed KSF. Half of the studied source areas are
129 breached in such a way that would allow full drainage (Fig. 2b, h). The other half are drained by channels
130 with a spill point that has a higher elevation than the source area floor (Fig. 3b, c), or are blocked by a
131 topographic obstacle (Fig. 2c, e) preventing complete drainage. Elevated mounds (<10 m high; e.g.
132 Fig. 2b, h) or linear ridges are located inside those source areas that are superposed on inclined surfaces.
133 These raised features, which are not visible in images from either CTX or HiRISE, are not connected
134 with the surrounding rims by elevated areas.

135 In five cases, a single kilometre-sized flow has emerged from the source area and spread over
136 the surrounding terrain. In one example multiple overlapping flows originate from the same source area
137 (Fig. 3a,c) forming a complex KSF. This complex KSF then develops a wide range of morphologies at
138 the distal parts of these flows: some flows have relatively steep margins, others show a smooth transition
139 into the surrounding terrain, or a sinusoidal depression surrounded by well-developed, but laterally
140 limited margins that stand from 10 to 15 meters above the bottom of this depression (Fig. 3a). The width
141 of the margins associated with this complex KSF shows that they are generally wider closer to the source
142 area than in the distal parts. However, there is an exception from this general trend. In one case, we
143 observed that the width as well as the height of the margins increased towards the end of KSF (see
144 position of dashed topographic profile on Fig. 3b and f).

145 Our observations support and refine previous findings by Komatsu et al. (2016) that suggested
146 the presence of two distinct types of margins at the flow edges. One type is characterized by scarps
147 (Fig. 2f) that are several metres high, whereas the other type has a smooth topographical transition into
148 the surrounding terrain and displays a distinct albedo contrast on visible data (i.e., on Fig. 3c marked as
149 bright units). The smooth transitions can be found either associated with discontinuities in meter-high
150 margins (Fig. 3d) or on the edges of small channels propagating on the meter-high margins (Fig. 3e).

151 The terrain over which the studied flows were emplaced is only slightly inclined (<6°), but steeper parts
152 are also present. The orientation of the flows reveals that the extruded material was moving downhill.

153 In one instance, we also observed ridge-like feature within the flow (Fig. 2c) as well as the
154 presence of a central channel within the flow surrounded by rims (Fig. 2j). On the other hand, we did
155 not observe the presence of large pits, rootless cones (i.e., constructional features caused by
156 accumulation of volcanic fragments resulting from water-lava interactions), subsidence or other signs
157 of violent explosions in association with source areas or at the margins of flows, which might be
158 expected for volcanic edifices.

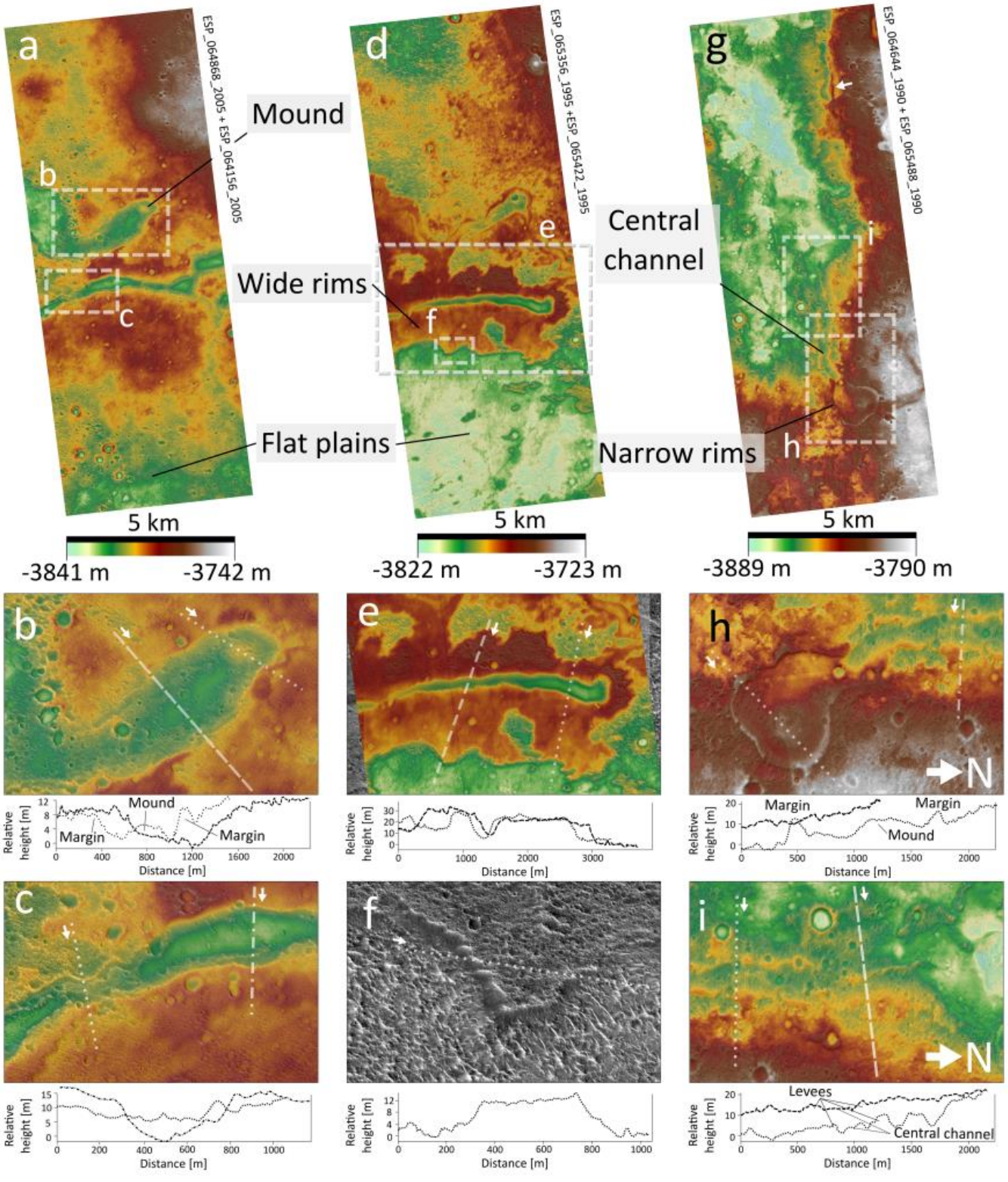

Figure 2: An example of three DEMs computed from HiRISE stereo pairs (a, d, g). For details about the used stereo-pairs see the description within the figure or Table 1. (b) Source area with well-developed central mound, breached towards SW; (c) A central channel; (e) Elongated source area

surrounded by kilometre-wide margins; (f) Margin of the flow, highlighting the different appearance of the flow-unit and the underlying terrain (HiRISE ESP_065356_1995); (h) Source area with well-developed mound, surrounded by distinct margins that are only few-hundred meters wide; (i) Middle part of the KSF with central channel (dashed and dashed-dotted lines mark the position of topographic profiles). Except for panels (h,i), north is towards the top of the images.

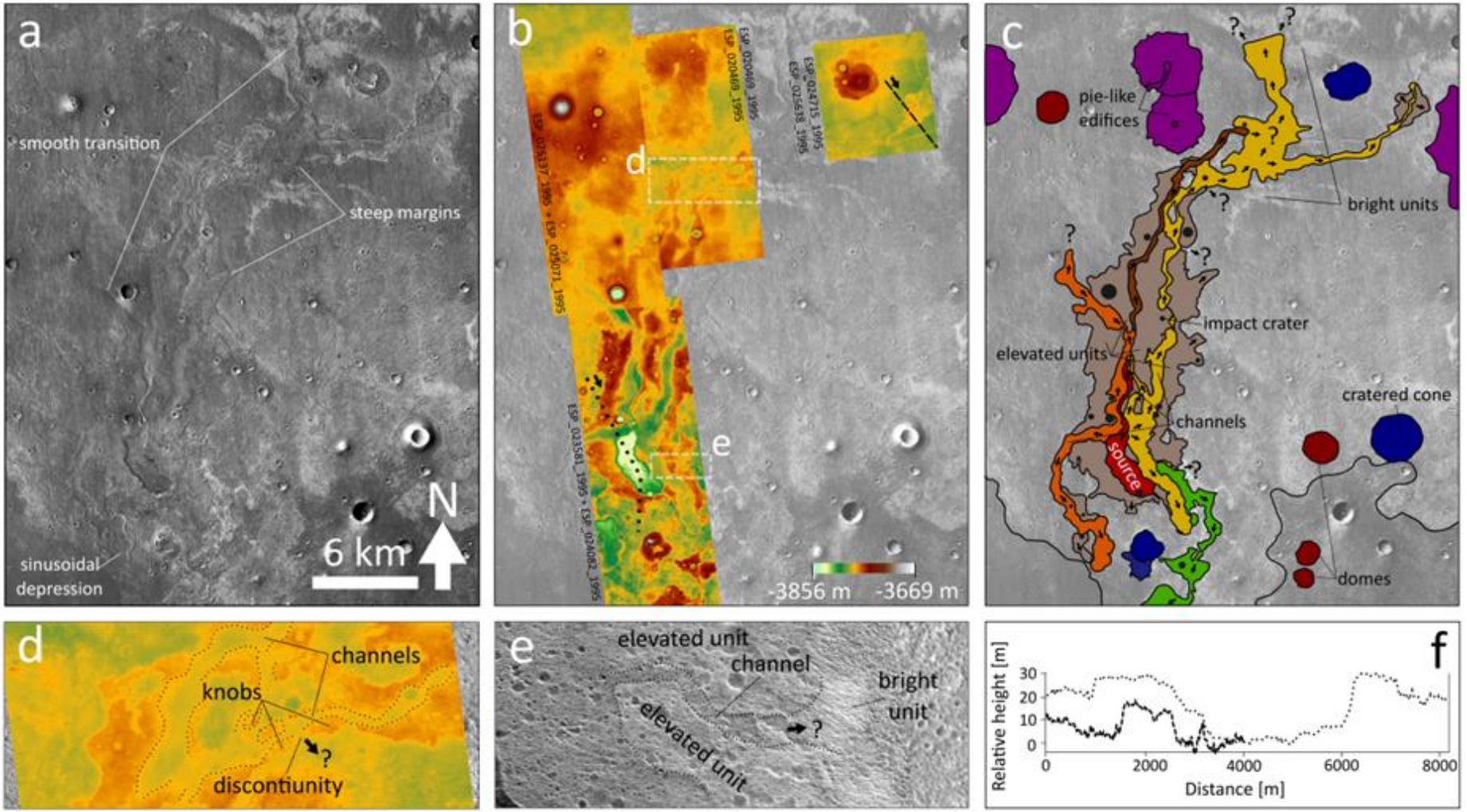
a
smooth transition
steep margins
sinusoidal depression
6 km
N
b
d
e
-3856 m
-3669 m
c
pie-like edifices
bright units
impact crater
elevated units
channels
source
cratered cone
domes
d
channels
knobs
discontiunity
e
elevated unit
channel
bright unit
elevated unit
f
Relative height [m]
Distance [m]
0
2000
4000
6000
8000
10
20
30

Figure 3: An example of multiple KSFs. (a) Several individual flows originating from a single source area (image: MurrayLab CTX mosaic, centred at 19.246°N, 322.78°E; Dickson et al., 2018); (b) Locations of 4 HiRISE DEMs together with the position of panels (d, e) and two topographic profiles shown on panel (f); (c) Simplified geomorphological sketch map marking the position of individual kilometre-sized flows together with the direction of the flow. Note the presence of associated dome-shaped, conical and pie-like edifices close to the KSF. Different colours denote individual observed flows and the small black arrows the proposed flow direction; (d) Discontinuity in the flow margins surrounding the branching central channel; (e) Detail of elevated unit forming flow margin that is intersected by small channels terminating at bright unit; (f) topographic profiles associated with dashed and dotted line in panel (b).

4 Discussion

4.1. Source areas

The inclination of the surfaces as well as the shape of source areas are consistent with the suggestion of Brož et al. (2019) that liquid material has been released from the source areas. Since the elevation of the source area floors is similar to that of the surrounding plains, this suggests that the liquid medium forming KSFs was emplaced directly onto the pre-existing surface from below. The topographic data additionally reveal that some source areas are not breached and instead a central channel-like feature with a floor that stands higher than the source area (Fig. 3b,c) emerges from them. These source areas are not as deep as those we interpret as being fully drained, their floors are relatively flat (see topographic profile on Fig. 3f) and no central mounds or large blocks or fractures are observed. This suggests that part of the material remained within these source areas, partly infilling them, and likely buried any positive relief present in the central part of the feeding vents. All source areas that seem to be fully drained do show the presence of mounds. These mounds are not morphologically consistent with results of mass wasting processes associated with rim collapses or with the remnants of subsidence of the source area's floor. Instead, based on their position within the source areas they appear to be the site where extruded material emerged at the surface.

These mounds cannot be identified on CTX or HiRISE visible images and are only revealed by using topography data obtained from HiRISE DEMs. As only seven HiRISE stereo-image pairs are

available over six KSFs, hence for a very small subset of the KSF population, we do not know how common such mounds really are within the entire KSF population in the southern part of Chryse Planitia. However, we consider it likely that the central mounds could be a common, yet inconspicuous feature of source areas of KSFs within the Chryse Planitia.

This conclusion is supported by the observation of terrestrial mud volcanoes where central mounds are relatively common (Fig. 4) and by the work of Komatsu et al. (2016) who noticed the presence of knobs with heights of several metres within the summit areas of dome-like edifices associated with KSFs within this area. The authors interpreted them as vent structures composed of accumulated sediment, like terrestrial gryphons or mud cones (for details about gryphons and their formation see Mazzini and Etiope, 2017). Later, Brož et al. (2019) studied a larger population of these domes and showed that these central knobs are common. They proposed an alternative formation scenario; expansion of the mud within the feeding conduit towards the end of the eruption induced by bubble growth due to the presence of boiling water (Hecht, 2002; Bargery et al., 2010). An analogous mechanism operating in magma has been previously proposed to explain the strange appearance of smooth mounds within Irregular Mare Patches on the Moon (Wilson and Head, 2017). The idea behind this process is that the low pressure causes expansion of gas bubbles trapped within the liquid (mud or lava), which extrudes a small amount of the remaining fluid from the feeding conduit (Wilson and Head, 2017, Brož et al., 2019). We propose that the central mounds reported here and the knobs within the summit areas of dome-like edifices could be produced by such a volumetric expansion.

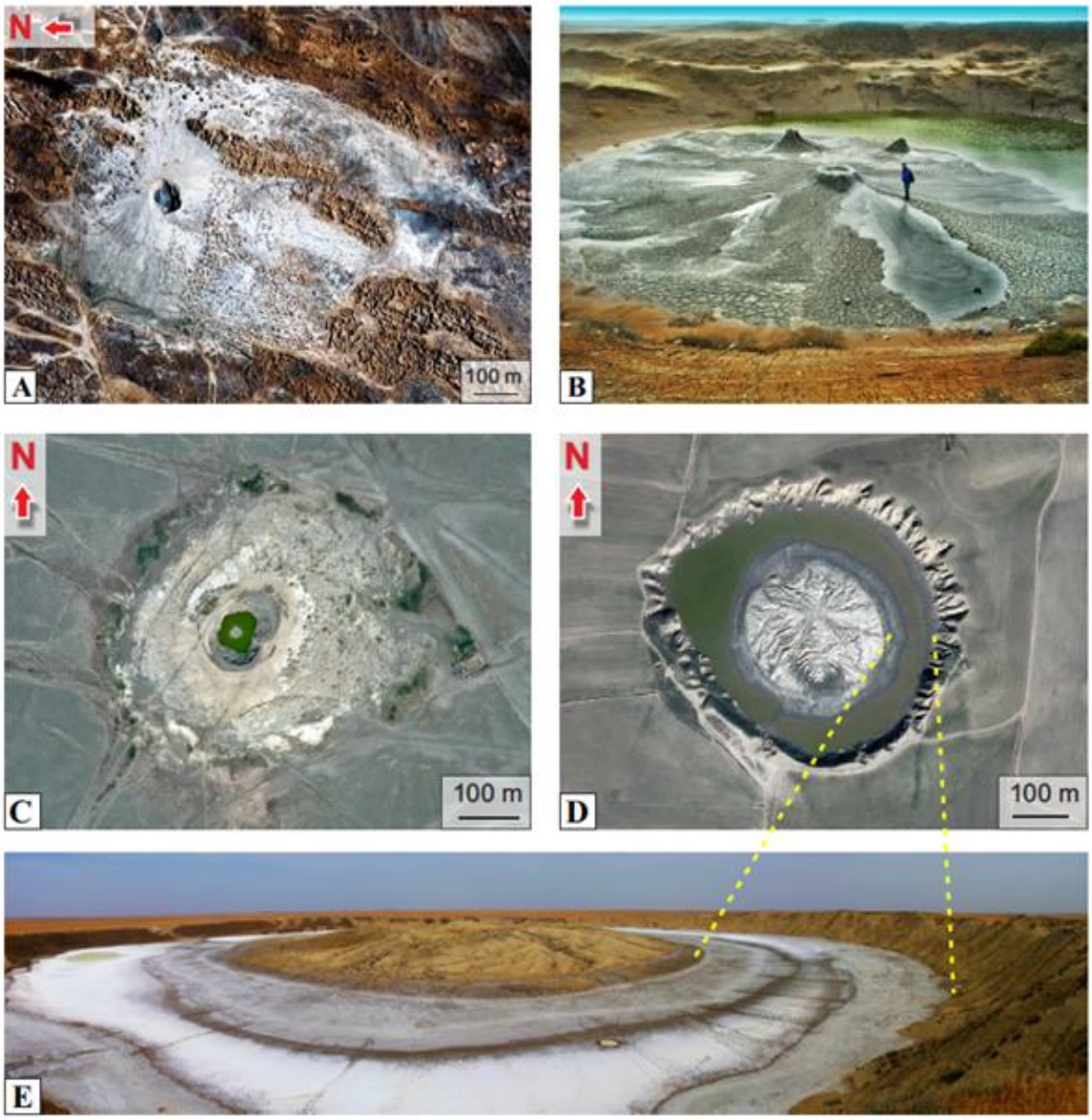

Fig. 4: Examples of low nearly flat sedimentary volcanoes on Earth where the floor of the crater has an elevation below that of the surroundings. A bulged morphology is often common in the central part of the crater floor (A, C, D are Google Earth satellite images). (A) Bahar Satellite MV, Azerbaijan, with very smooth surface texture and low elevation and central subsided crater. (B) Field view inside the Bahar Satellite MV crater where active gryphons and pools located in the central bulge release gas and mud. (C) Naftliche MV, Iran hosting a lake and a bulge in the central crater where gas and water seepages occur. (D) Gharniarigh MV, Iran, showing a distinct isolated island inside the crater. (E) Field

view of Gharniarigh MV, showing the central bulge. When the water filling the crater evaporates, the area around the bulge features thick salt deposits originating from the seeping brines.

Alternatively, the central mounds could also have formed by the ascent of more viscous material during the very late stage of the eruption caused by the partial depletion of the volatile source of the liquid. Under such a scenario, we envisage that the viscosity of the mud, and hence its ability to propagate, may vary during the course of eruption. At the beginning, low viscosity water-rich mud could be released. Such mud would be mobile and capable of propagating to significant distances. As the mud continues to be released, the eruption wane and the viscosity of the mud may change. Under such a scenario, different viscosities of mud would form the domes and the KSFs. Further, viscosity contrasts could explain why knobs occur in some constructs and mounds in others. Higher viscosity mud would be associated with steeper and better recognizable knobs, while lower viscosity mud would instead produce wider and less visible mounds.

It remains unclear whether mounds associated with KSFs are the result of the ascent of more viscous material, due to the bubble growth, or combination of these processes, but in both cases these mounds would represent the surface expressions of the feeding conduits. However, as these mechanisms can occur both during lava as well as mud effusions, the presence of the mounds themselves cannot be used as diagnostic evidence to favour sedimentary volcanism over igneous volcanism. Nevertheless, it can be used as clear evidence supporting the extrusion of material from the subsurface. Our observations hence complement previous works (Komatsu et al., 2016, Brož et al., 2019), suggesting that KSFs are aggradational features formed by the transport of a fluid. This conclusion is additionally supported by our observations of the rims around the source areas – while some are only dozens of meters wide, others reach a width up to several kilometres. Our observations suggest that the slope of surrounding terrain is responsible for these variations. Rims situated on relatively flat surroundings are wider than those situated on an inclined surface. This again highlights that the material was extruded from the source areas and spread into the surroundings by following the topographic gradient. However, in one case, we observed that one of the studied north-south oriented flows has the western edge at lower elevation than

the eastern one (Fig. 2i and associated topographic profiles). Such imbalance in the flow edge elevation suggests that the terrain over which the flow moved may have partly subsided after the flow's emplacement and points to subsequent deformation of the surface.

4.2. Flow margins

We were able to confirm the observations of Komatsu et al. (2016), who identified two distinct types of margins at the flow edges. We also observed that those surrounding the central large channels are not continuous. They are often breached by meter-sized channels linking the central one to the bright units (Fig. 3e), or alternatively, by troughs in the margins enabling the propagation of material from the central channels to the surroundings (Fig. 3d). While meter-sized channels are relatively shallow and hence they do not cut through the entire thickness of accumulated deposits. The troughs have the same elevation as surrounding units suggesting that part of the margin was removed completely. In both cases, no significant material accumulation was measurable in these areas of distinct brightness. This shows that the fluid medium was capable of a dual behaviour: a) form elevated margins and b) also propagate into the surroundings without displaying defined topographical boundaries at the surface. The main evidence of these deposits is the resulting surficial expression indicated by brightness variations at the surface. Such expression is unlikely to be related to igneous deposits, even in the case of very low viscosity lavas. This is because once lava is released from the main channel, it would rapidly solidify due to the heat loss. Hence, it would form a relatively resistant unit that should leave a topographic relief, which is not observed. Therefore, the absence of such resistant unit suggests that the media that ran out from these small channels and troughs behaved differently from lava. The deposited material had to be easily erodible and could later be transported from these bright units by some other mechanism(s).

Additionally, the presence of a sinusoidal depression associated with the complex KSF marked on Fig. 3a supports a high erodibility and/or an additional transport of the effused fluid after the emplacement. This sinusoidal depression is surrounded by margins standing 10 to 15 meters above the bottom of this depression. This suggests that the incoming material was able to reach such heights, but later was removed or withdraw elsewhere. As no outgoing channel(s) is observed, it is unlikely that the

material flowed out of the depression. If lava had flowed through the channel, it would accumulate within such depression and leave some relict evidence that could be observed today, even if the lava flow would partly subside after cooling and solidification and hence decrease its volume. However, at the same time, released fluid has to be also capable of forming topographically positive landforms on the flow edges as indicated by the topographic profile on Fig. 3h with a dashed line.

To explain these observations, we therefore propose a scenario that involves the release of large volumes subsurface water-rich sediments that could modify the surface morphology and spread over a broad area. It remains unclear whether the transport of such media was accompanied by evaporative cooling leading to the formation of a protective icy-muddy crust (Brož et al., 2020) as the environmental properties at the time of eruption are currently unknown. However, it should be considered that when such mixture spreads over a wide area, the water may infiltrate into the subsurface if the thermal conditions of the subsurface are favourable (Stähli et al., 1999). Alternatively, liquid water could evaporate into the atmosphere, or the water-mud mixture could completely freeze and later the ice could be removed by sublimation (Bargery et al., 2010; Brož et al., 2020a) leaving behind a rougher and hence brighter surface. Independent of whether sublimation, evaporation, infiltration or a combination of these processes was the dominant factor responsible for the water loss, the water would be lost without leaving a detectable topographic expression, leaving instead a change in the roughness of the surface and hence in the surface albedo.

However, it should be noted that when the water-rich mixture moved through narrow topographic depressions, the transported sediment was able to leave deposits on the edges of the flows and flow margins were formed. As a result, further movement was channelized and levees gradually formed around them. As the amount of effused water-rich mud would not be stable over the course of the entire eruption, this might cause overspills and hence a formation of laterally extensive margins. Such mechanism is known from terrestrial floodplains where the water is capable to deposit the carried sediments outside of the main channel during floods and hence form levees and distant layers of sediments (Junk et al., 1989; Bedient et al., 2008; Syvitski et al., 2012).

Our observations do not reveal any evidence that favours igneous volcanism over sedimentary volcanism. We do not observe signs of subsidence or explosive excavation, which are often present if features were formed by magmatic eruptions (e.g., Sheridan and Wohletz, 1983; Wohletz and Sheridan, 1983; Lorenz, 1986; Brož and Hauber, 2013). We also did not find any signs of explosive activity on the edges of observed KSFs or the presence of rootless cones that often accompany lava flows in other areas of Mars where subsurface volatiles are present (e.g., Fagents and Thordarson, 2007). It remains unclear whether volatiles were present in the subsurface during the period when the studied KSFs formed and if yes, at what depth(s), but the presence of rampart craters within the study area (e.g., Barlow and Perez, 2003; Reiss et al., 2006) argues for their past presence. The combined observations provide support of sedimentary volcanism over igneous volcanism. However, it should be stressed that individual isolated evidence cannot be used alone as an argument to reject igneous volcanism. This is because explosive features or signs of subsidence do not necessarily form at all effusive igneous eruptions, and/or they could be hidden or modified by subsequent resurfacing processes beyond recognition. Without ground truth data, therefore, the igneous scenario cannot be ruled out. Nevertheless, our observations provide new evidence to support the hypothesis previously proposed by Komatsu et al. (2016) and later supported by Brož et al. (2019) that these studied KSFs were formed by subsurface sediment mobilization. While the central mounds can be explained by igneous as well as sedimentary volcanism, the presence of bright units associated with the release of the fluid from the main channels and the presence of sinusoidal depression would be challenging to explain by the movement of lava.

4.3. Implications

As previously stated, the KSFs are not the only features within the southern part of Chryse Planitia that have been proposed to be formed by subsurface sediment mobilization (Komatsu et al., 2016; Brož et al., 2019). They are accompanied by conical, dome-shaped, and pie-like edifices of various shapes and sizes, and a genetic connection between these types can be explored. Our study shows that the southern part of Chryse Planitia is a region on Mars hosting a large variety of morphological shapes (domes, cones or KSFs) potentially connected to sedimentary eruptions, whereas other fields of putative

sedimentary edifices show larger uniformity in their populations (e.g., Skinner and Tanaka, 2007; Okubo, 2016, Cuřín et al., 2021). For example, the extensive field of edifices within Coprates Chasma shows the presence of pitted cones and associated sub kilometre flows that could be sedimentary (Okubo, 2016) or igneous in origin (Brož et al., 2017), but large KSFs are missing. In contrast, the field of edifices in Adamas Labyrinthus investigated by Ivanov et al. (2017) and Cuřín et al. (2021) shows more than 200 KSFs, but a frequent occurrence of pitted kilometre-sized cones and domes was not observed. These KSFs were interpreted in both studies as being large mud flows formed due to the ascent of a low viscosity mixture of water and sediment. Another large field of kilometre-sized pitted cones in the Nepenthes/Amenthes region, whose origin has been interpreted as either sedimentary (Skinner and Tanaka, 2007) or igneous (Brož and Hauber, 2013), does not show the presence of well-developed KSFs, domes or pie-like edifices. The large variability in the shapes of different edifices in Chryse Planitia suggests that the extruded material had a relatively wide range of viscosities spanning from very low viscosity and hence water-dominated mixtures that formed the studied KSFs, up to relatively viscous mixtures that were unable to move over large distances and hence formed the domes (Brož et al., 2019).

We also note that the studied KSFs (Fig. 5a) are very different in appearance from other putative martian kilometre-sized mud flows proposed to be formed by low viscosity muds, such as those situated in Adamas Labyrinthus (Fig. 5b, Cuřín et al., 2021) or the unique 40 km-long flow of Zephyria Fluctus (Fig. 5c, Wilson and Mouginis-Mark, 2014). Flows in both areas are characterized by smooth central uplifted plateaus usually surrounded by a topographically lower boundary formed by an assemblage of lobes or hummocks. However, while uplifted units in Adamas Labyrinthus do not show any flow-like expressions on their surfaces, the flow of Zephyria Floctues shows very clear signs of fluid flow in a laminar fashion (Wilson and Mouginis-Mark, 2014). It remains unclear why such significant variations in shapes and appearances among putative mud KSFs from different regions exist. Different environmental properties, namely atmospheric pressure and temperature of the atmosphere or the surface, might have played a role. Experimental studies (Brož et al. 2020a,b) showed that variations in these parameters may have a profound effect on the way the mud propagates as well as its ability to

remain in a liquid phase under reduced martian atmospheric pressure. As these KSFs have been formed in different martian regions and possibly also in different epochs (Ivanov et al., 2016; Brož et al., 2019), these parameters may have varied significantly and hence have an impact on the resulting shapes of these features. Unfortunately, this quandary remains unanswered for the conditions of the studied KSFs in Chryse Planitia, since the investigation of their morphologies and morphometries did not provide any evidence regarding the manner in which the water-rich mud propagated over the surface. Similarly, these factors also remain unknown for other regions. These variations among putative martian mud flows stress the need to develop numerical models capable of simulating how different environmental properties may influence the morphology of resulting sedimentary edifices and flows.

Our observations add to the recognition that subsurface sediment mobilization is a potentially significant process shaping several regions of the martian surface (e.g., Skinner and Tanaka, 2007; Skinner and Mazzini, 2009; Okubo, 2016; Komatsu et al., 2016; Ivanov et al., 2017; Hemmi and Miyamoto, 2017, 2018; Di Pietro et al., 2021). These regions are not all identical in theirgeologic settings, hence it should not be expected that all surface manifestations of sedimentary volcanism are morphologically similar. The depocenters that would host the source reservoirs have different sizes, the sediments would have been sourced from different lithologies and by different processes, and even the conditions (e.g., density stratification, overpressurization) that triggered the liquefaction and mobilization would likely have been different.

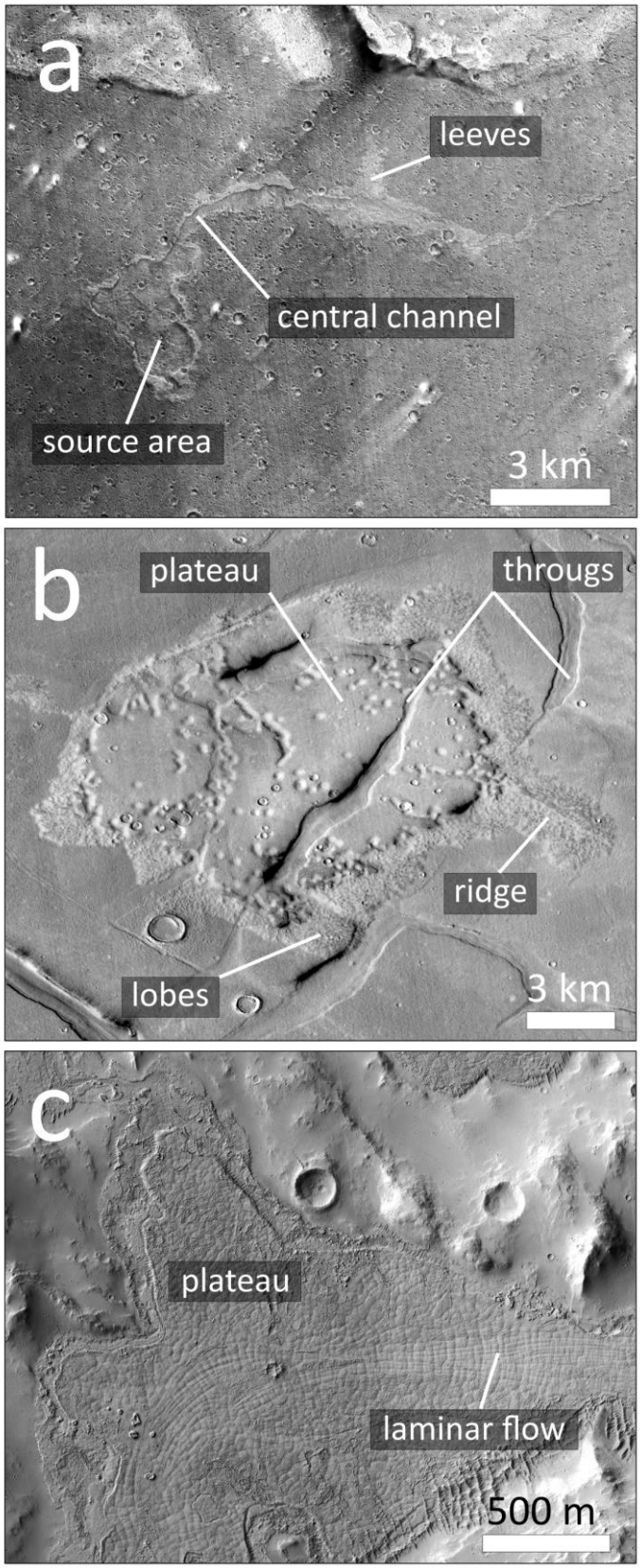

377

378 Figure 5: A compilation capturing three typical examples of low viscosity KSFs from different
379 regions of Mars proposed to be sedimentary in origin. a) KSFs at Chryse Planitia typically show a

source area, a central channel as well as well-developed levees (based on Murray Beta CTX mosaic, Dickson et al., 2018; centred 19.87°N, 325.93°E); b) KSF in Adamas Labyrinthus are characterized by smooth central uplifted plateaus surrounded by an assemblage of lobes. (based on Murray Beta CTX mosaic, Dickson et al., 2018;; centred 39.14°N, 100.93°E); c) 40-km long flow of Zephyria Fluctus has a very distinct surficial expression as flow patterns can be clearly recognized (based on HiRISE image ESP_027464_1805; centred 0.65°N, 155.39°E).

For example, if the edifices studied by Okubo (2016) are indeed sedimentary volcanoes, their source reservoir inside the extensional tectonic structure of Valles Marineris would likely be smaller, and the accumulation process would have been different from those in Chryse Planitia, which are located in a huge ancient impact crater and were accumulated by the transport processes that shaped the outflow channels. It is equally unlikely that the water content in the source reservoirs of all possible sedimentary volcanoes on Mars would have been similar, let alone identical. Specifically, the accumulation of sediments through the circum-Chryse outflow channels would lead to the heterogeneous accumulation of subsurface deposits at different depths that are expected to be variable in composition and water content. The extrusion of mud from one or several of these reservoirs would be expected to generate a greater variety of surface features with morphological differences higher than those n encountered in regions with a more uniform source reservoir.

We therefore ascribe the observed morphological diversity of sedimentary volcanism-related landforms in southern Chryse Planitia to a correspondingly large variability of the source reservoir properties, and the studies KSFs would represent features that form by relatively small-volume eruptions of water-rich sediments. As these surface deposits bear a record of exchange processes between the deep, volatile-rich subsurface and the surface, they are very attractive targets for the exploration of past sedimentary processes and possibly associated subsurface habitats.

5 Conclusions

Our study reveals that the morphology of KSFs in Chryse Planitia is consistent with the flow of low-viscosity and hence water-rich mud across the martian surface. Based on the observed morphologies

of the studied KSFs it is possible to identify the source area from which the mud was extruded from the subsurface. Once erupted, the transported sediment was deposited on the edges of the flows when its yield strength was sufficiently high, and flows margins were formed. This formed a central channel with leveed margins of various widths. Once the flow event terminated, the infiltration of water into the subsurface and/or sublimation of ice removed substantial volumes from the terminal parts of the flows thus explaining some of the observed morphologies associated with the terminal edges and shapes of source areas. Our findings strengthen the hypothesis proposed by Komatsu et al. (2016) and Brož et al. (2019) that these features are martian mud flows, formed by subsurface sediment mobilization as opposed to igneous volcanism. Hence, these features represent an open window to the subsurface and are interesting targets for in-situ analyses to access and investigate buried deposits (Komatsu and Brož, 2021) that are beyond our reach with the current technology.

6 Acknowledgments

PB & YM were supported by Czech Science Foundation (#20-27624Y). SJC & AN are supported by the French Space Agency CNES for their HiRISE related work. AM is supported by the Research Council of Norway (#223272-288299). PW was supported during the project by the UK Space Agency (#ST/L006456/1).

7 References

Bargery, A.S., Lane, S.J., Barrett, A., Wilson, L., Gilbert, J.S., 2010. The initial responses of hot liquid water released under low atmospheric pressures: experimental in-sights. Icarus 210 (1), 488–506. https://doi.org/10.1016 /j.icarus.2010.06.019.

Barlow, N. G., Perez, C. B., 2003. Martian impact crater ejecta morphologies as indicators of the distribution of subsurface volatiles, J. Geophys. Res., 108(E8), 5085. https://doi.org/10.1029/2002JE002036.

Bedient, P.B., Huber, W.C., Vieux, B.E., 2008. Hydrology and floodplain analysis, Prentice Hall Upper Saddle River, NJ.

Bleacher, J.E., Greeley, R., Williams, D.A., Cave, S.R., Neukum, G., 2007. Trends in effusive style at the Tharsis Montes, Mars, and implications for the development of the Tharsis province. J. Geophys. Res. 112, E09005. doi:10.1029/2006JE002873.

Burrough, P. A., and McDonell, R. A., 1998. Principles of Geographical Information Systems (Oxford University Press, New York), 190 pp.

Brož, P., Hauber, E., 2013. Hydrovolcanic tuff rings and cones as indicators for phreatomagmatic explosive eruptions on Mars. Journal of Geophysical Research: Planets, 118, 1656–1675. https://doi.org/10.1002/jgre.20120

Brož, P., Hauber, E., Wray, J. J., Michael, G., 2017. Amazonian volcanism inside Valles Marineris on Mars. Earth and Planetary Science Letters 473, 122–130, doi:10.1016/j.epsl.2017.06.003.

Brož, P., Hauber, E., van de Burgt, I., Špillar, V., Michael, G., 2019. Subsurface sediment mobilization in the southern Chryse Planitia on Mars. J. Geophys. Res., Planets 124. https://doi .org /10 .1029 /2018JE005868.

Brož, P., Krýza, O., Wilson, L., Conway, S. J., Hauber, E., Mazzini, A., Raack, J., Patel, M. R., Balme, M. R., Sylvest, M. E., 2020a. Experimental evidence for lava-like mud flows under Martian surface conditions. Nature Geoscience. https://doi.org/10.1038/s41561-020-0577-2.

Brož, P., Krýza, O., Conway, S. J., Mueller, N. T., Hauber, E., Mazzini, A., Raack, J., Patel, M. R., Balme, M. R., Sylvest, M. E., 2020b. Mud Flow Levitation on Mars: Insights from Laboratory Simulations. EPSL 545. https://doi.org/10.1016/j.epsl.2020.116406.

Cuřín, V., Brož, P., Hauber, E., Markonis, Y., 2021. Mud flows in the Southwestern Utopia Planitia, Mars. EPSC conference, Vol. 15, EPSC2021-382.l.

452 Dickson, J.L., Kerber, L.A., Planetary, C.F.L.A., 2018. A global, blended CTX mosaic of Mars with
453 vectorized seam mapping: A new mosaicking pipeline using principles of non-destructive image editing.
454 49th Lunar and Planetary Science Conference, #2480.

455 Di Pietro, I.. Séjourné, A., Costard, F., Ciążela, M., Palmero Rodriguez, J. A. 2021. Evidence of mud
456 volcanism due to the rapid compaction of martian tsunami deposits in southeastern Acidalia Planitia,
457 Mars. Icarus 354, 114096. https://doi.org/10.1016/j.icarus.2020.114096.

458 Fagents, S.A., Thordarson, T., 2007. Rootless volcanic cones in Iceland and on Mars. In: Chapman, M.
459 (Ed.), The Geology of Mars. Cambridge University Press. Cambridge, United Kingdom, pp. 151–177.

460 Hauber, E., Bleacher, J., Gwinner, K., Williams, D., Greeley, R., 2009. The topography and morphology
461 of low shields and associated landforms of plains volcanism in the Tharsis region of Mars. J. Volcanol.
462 Geotherm. Res. 185, 69–95. https://doi.org/10.1016/j.jvolgeores.2009.04.015.

463 Hecht, M.H., 2002. Metastability of liquid water on Mars. Icarus 156, 373–386.
464 https://doi.org/10.1006/icar.2001.6794.

465 Hemmi, R., Miyamoto, H., 2017. Distribution, morphology, and morphometry of circular mounds in the
466 elongated basin of northern Terra Sirenum, Mars. Progress in Earth and Planetary Science 4:26.
467 https://doi.org/10.1186/s40645-017-0141-x.

468 Hemmi, R.; Miyamoto, H. 2018. High-Resolution Topographic Analyses of Mounds in Southern
469 Acidalia Planitia, Mars: Implications for Possible Mud Volcanism in Submarine and Subaerial
470 Environments. Geosciences 8, 152. https://doi.org/10.3390/geosciences8050152.

471 Hodges, C.A., Moore, H.J., 1994. Atlas of volcanic features on Mars. U. S. Geol. Survey Professional
472 Paper 1534. U. S. Govt. Printing Office, Washington DC, p. 194.

473 Ivanov, M. A., Erkeling, G., Hiesinger, H., Bernhardt, H., Reiss, D. 2017. Topography of the
474 Deuteronilus contact on Mars: Evidence for an ancient water/mud ocean and long-wavelength

475 topographic readjustments. Planetary and Space Science, 144, 49–70.
476 https://doi.org/10.1016/j.pss.2017.05.012.

477 Junk, W. J., Bayley, P. B., Sparks, R. E., 1989. The flood pulse concept in river-floodplain systems:
478 Canadian special publication of fisheries and aquatic sciences, v. 106, no. 1, p. 110-127.

479 Keszthelyi, L. et al., 2008. High Resolution Imaging Science Experiment (HiRISE) images of volcanic
480 terrains from the first 6 months of the Mars Reconnaissance Orbiter primary science phase. J. Geophys.
481 Res. 113, E04005. doi:10.1029/2007JE002968.

482 Kirk, R. L., Howington-Kraus, E., Rosiek, M. R, et al., 2008. Ultrahigh Resolution Topographic
483 Mapping of Mars with MRO HiRISE Stereo Images: Meter-Scale Slopes of Candidate Phoenix Landing
484 Sites. Journal of Geophysical Research, 113(E12): E00A24. https://doi.org/10.1029/2007je003000

485 Komatsu, G., Okubo, C.H., Wray, J.J., Ojha, L., Cardinale, M., Murana, A., Orosei, R., Chan, M.A.,
486 Ormö, J., Gallagher, R., 2016. Small edifice features in Chryse Planitia, Mars: assessment of a mud
487 volcano hypothesis. Icarus 268, 56–75. https://doi.org/10.1016/j.icarus.2015.12.032.

488 Komatsu, G., Brož, P., 2021. Southern Chryse Planitia on Mars as a Potential Landing Site: Investigation
489 of Hypothesized Sedimentary Volcanism. LPSC2021, #1164.

490 Lorenz, V., 1986. On the growth of maars and diatremes and its relevance to the formation of tuff rings,
491 Bull. Volcanol., 48, 265–274. https://doi.org/10.1007/BF01081755.

492 Malin, M. C., Bell, J. F. III, Cantor, B. A., Caplinger, M. A., Calvin,W. M., Clancy, R. T., et al., 2007.
493 Context camera investigation on board the Mars Reconnaissance Orbiter. Journal of Geophysical
494 Research, 112, E05S04. https://doi.org/10.1029/2006JE002808.

495 Mazzini, A., Etiope, G., 2017. Mud volcanism: An updated review. Earth-Science Reviews, 168, 81–
496 112. https://doi.org/10.1016/j.earscirev.2017.03.001.

497 McEwen, A. S., Eliason, E. M., Bergstrom, J. W., Bridges, N. T., Hansen, C. J., Delamere, W. A., et al.,
498 2007. Mars Reconnaissance Orbiter's High Resolution Imaging Science Experiment (HiRISE). Journal
499 of Geophysical Research, 112, E05S02. https://doi.org/10.1029/2005JE002605.

500 Moratto, Z. M., Broxton, M. J., Beyer, R. A., Lundy, M., Husmann, K., 2010. Ames stereo pipeline,
501 NASA's open source automated stereogrammetry software, In 41st Lunar and Planetary Institute
502 Science Conference, Abstract 2364.

503 Okubo, C.H., 2016. Morphologic evidence of subsurface sediment mobilization and mud volcanism in
504 Candor and Coprates Chasmata, Valles Marineris, Mars. Icarus 269, 23–27.
505 https://doi.org/10.1016/j.icarus.2015.12.051.

506 Reiss, D., Gasselt, S., van, Hauber, E., Michael, G., Jaumann, R., Neukum, G., 2006. Ages of rampart
507 craters in equatorial regions on Mars: implications for the past and present distribution of ground ice.
508 Meteorit. Planet. Sci. 41, 1437–1452. https://doi.org/10.1111/j.1945-5100.2006.tb00428.x.

509 Sheridan, M. F., Wohletz, K. H., 1983. Hydrovolcanism: Basic considerations and review, J. Volcanol.
510 Geotherm. Res., 17, 1–29. https://doi.org/10.1016/0377-0273(83)90060-4.

511 Skinner, J. A., Tanaka, K. L., 2007. Evidence for and implications of sedimentary diapirism and mud
512 volcanism in the southern Utopia highland-lowland boundary plain, Mars. Icarus, 186(1), 41–59.
513 https://doi.org/10.1016/j.icarus.2006.08.013.

514 Skinner, J. A., Mazzini, A., 2009. Martian mud volcanism: Terrestrial analogs and implications for
515 formational scenarios, Mar. Pet. Geol., 26(9), 1866–1878.
516 https://doi.org/10.1016/j.marpetgeo.2009.02.006.

517 Stähli, M., Jansson, P.-E., Lundin, L.-C., 1999. Soil moisture redistributionand infiltration in frozen
518 sandy soils. Water Resources Research,35(1),95–103. https://doi.org/10.1029/1998WR900045.

519 Syvitski, J. P., Overeem, I., Brakenridge, G. R., Hannon, M., 2012. Floods, floodplains, delta plains—a
520 satellite imaging approach: Sedimentary Geology, v. 267, p. 1-14.
521 https://doi.org/10.1016/j.sedgeo.2012.05.014.

522 Tanaka, K. L., Skinner, J. A. Jr., Hare, T. M., 2005. Geologic map of the northern plains of Mars, U.S.
523 Geological Survey Scientific Investigations Map SIM-2888, Scale 1:15,000,000.

524 Wilson, L., Head, J. W., 2017. Eruption of magmatic foams on the Moon: Formation in the waning
525 stages of dike emplacement events as an explanation of "irregular mare patches". Journal of
526 Volcanology and Geothermal Research, 335, 113–127.
527 https://doi.org/10.1016/j.jvolgeores.2017.02.009.

528 Wilson, L., Mouginis-Mark, P.J., 2014. Dynamics of a fluid flow on Mars: lava or mud? Icarus 233,
529 268–280. https://doi.org/10.1016 /j.icarus.2014.01.041.

530 Wohletz, K. H., Sheridan, M. F., 1983. Hydrovolcanic explosions II. Evolution of basaltic tuff rings and
531 tuff cones, Am. J. Sci., 283, 385–413. https://doi.org/10.2475/ajs.283.5.385.